Influence of Nitrogen Base Ligation on the Rate of Reaction of [5,10,15,20-Tetrakis(2,6-dimethyl-3-sulfonatophenyl)-porphinato]iron(III) Hydrate with *t*-BuOOH in Aqueous Solution[1]

Michael J. Beck, Enona Gopinath, and Thomas C. Bruice*

Contribution from the Department of Chemistry, University of California at Santa Barbara, Santa Barbara, California 93106. *Received April 9, 1992*

Abstract: In aqueous solution, the axial ligands of [5,10,15,20-tetrakis(2,6-dimethyl-3-sulfonatophenyl)porphinato]iron(III) are water and/or hydroxide ion [(**1**)$Fe^{III}(OH_2)_2$, (**1**)$Fe^{III}(OH_2)(OH)$, and (**1**)$Fe^{III}(OH)_2$; (pK_{a1} = 6.75, $pK_{a2} \cong$ 10.8]. Hydroperoxide reduction occurs via axial ligation of hydroperoxide to form the complexes (**1**)$Fe^{III}(OH_2)$(HOOR), (**1**)$Fe^{III}(OH_2)$(OOR), and (**1**)Fe^{III}(OH)(OOR). In the pH ranges 4–8 with $CF_3CH_2NH_2$ (pK_a = 5.70) and 6–10 with NH_3 (pK_a = 9.24) and imidazole (pK_a = 6.95), the nitrogen base ligated iron(III) porphyrin species are (**1**)$Fe^{III}(OH_2)$(Am), (**1**)$Fe^{III}(Am)_2$, and (**1**)Fe^{III}(OH)(Am) (Scheme I). We have established that mono nitrogen base ligation to form the complex (**1**)$Fe^{III}(OH_2)$(Am) results in a rate enhancement, whereas bis ligation to form the complex (**1**)$Fe^{III}(Am)_2$ inhibits the reaction. Thus hydroperoxide reduction by iron(III) porphyrin must occur via axial ligation of hydroperoxide. As the extinction coefficients for the mono nitrogen base ligated species [ϵ_{1N} for (**1**)$Fe^{III}(OH_2)$(Am) and ϵ_{2N} for (**1**)Fe^{III}(OH)(Am)] are unknown, the equilibrium constants for the formation of nitrogen base ligated iron(III) porphyrin were calculated using a wide range of plausible values for ϵ_{1N} and ϵ_{2N}. The calculated equilibrium constants for formation when Am = NH_3 are K_{N1} = (0.1–1.5) × 10^2 M^{-1} for (**1**)$Fe^{III}(OH_2)$(Am) and $\beta = K_{N1}K_{N2}$ = (4.4–8.4) × 10^4 M^{-2} for (**1**)$Fe^{III}(Am)_2$. When Am = imidazole, K_{N1} = (1–5) × 10^3 M^{-1} and β = (5–8) × 10^8 M^{-2}. With $CF_3CH_2NH_2$ equilibrium constants are much lower, so that sufficient concentrations of $CF_3CH_2NH_2$ for the determination of K_{N1} and K_{N2} could not be reached. Kinetic studies of the pH dependence for the reaction of the iron(III) porphyrin with *t*-BuOOH in the presence of $CF_3CH_2NH_3^+/CF_3CH_2NH_2$, $(NH_4^+/NH_3$, and imidazole·H^+/imidazole were carried out using disodium 2,2′-azinobis(3-ethylbenzthiazolinesulfonate) as a trap to follow the turnover of the iron(III) porphyrin catalyst. It was established that NH_3 does not serve as a substrate for oxidation by iron(IV)–oxo porphyrin species. The equilibrium constant K_{N1} for the formation of (**1**)$Fe^{III}(OH_2)$(imidazole) is 10^1–10^2-fold larger than for formation of (**1**)$Fe^{III}(OH_2)(NH_3)$, while the equilibrium constant $K_{N1}K_{N2}$ for ligation of imidazole to form the inert (**1**)Fe^{III}(imidazole)$_2$ is 10^4-fold greater than $K_{N1}K_{N2}$ to form (**1**)$Fe^{III}(NH_3)_2$. Thus when Am = NH_3 or $CF_3CH_2NH_2$, (**1**)$Fe^{III}(OH_2)$(Am) accumulates to a kinetically significant extent at low [Am] before enough of the unreactive (**1**)$Fe^{III}(Am)_2$ builds up to inhibit the reaction, but when Am = imidazole the converse is true. Therefore, addition of low concentrations of NH_3 or $CF_3CH_2NH_2$ enhances the reaction of the iron(III) porphyrin with *t*-BuOOH, while the addition of imidazole does not produce a rate enhancement. The ratio of the second-order rate constants for the reactions of (**1**)$Fe^{III}(OH_2)(NH_3)$/(**1**)$Fe^{III}(OH_2)_2$ with *t*-BuOOH was calculated to be between 1.4 × 10^3 and 1 × 10^5, while that for the reactions of (**1**)$Fe^{III}(OH_2)(NH_3)$/(**1**)$Fe^{III}(OH_2)$(OH) with *t*-BuOOH was calculated to be between 10 and 10^3, dependent upon the choice of ϵ_{1N} and ϵ_{2N}. These ratios represent, in part, the favorable electron donor capacity of ammonia as compared to water.

Introduction

Variations in the protein environment of the iron protoporphyrin cofactor in the enzymes peroxidase, catalase, and cytochrome P-450 allow widely varying enzymatic reactions. In each of these enzymes the cofactor is axially ligated to a basic amino acid side chain at the face opposite to which the catalytic reaction involving the iron moiety occurs. Thus, in peroxidases the nitrogen base of a histidine imidazole acts as axial ligand, catalases have the oxygen base of a tyrosine phenoxide as axial ligand, and cytochrome P-450 enzymes have the thiol anion of a cysteine as axial ligand.[2] The state of axial ligation to the iron porphyrin cofactor is an important structural feature controlling the reactivity of the enzyme.

The binding of ammonia[3,4] and alkyl-[4,5] and arylamines[4,6–9] to iron(III) porphyrins has been extensively investigated. The ligation of a nitrogen base to an iron(III) porphyrin occurs in two steps, with initial monoligation to form a high-spin iron(III) porphyrin complex (eq 1a), followed by further ligation of nitrogen base to the opposite face to form the low-spin, bis-ligated complex (eq 1b). In most cases $K_2 \gg K_1$, such that only the low-spin, bis

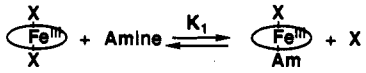

(1a)

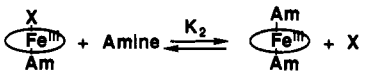

(1b)

nitrogen base ligated complexes are observed.[3–5,8] In the special cases involving titration of iron(III) porphyrin with 2-methyl- or *N*-methylimidazole, UV–vis spectra provided evidence for the accumulation of intermediate mono-ligated complexes prior to bis ligation.[6,7] In analogous studies performed with imidazole, however, no evidence for the accumulation of mono-ligated species was observed.[6,7] The bis nitrogen base complexes of iron(III) porphyrins cannot ligate hydroperoxides, because both axial ligand positions are occupied by nitrogen base. Thus, no catalysis of hydroperoxide cleavage by iron(III) porphyrin can be observed at high concentrations of imidazole.

In the case of manganese porphyrins, only mono nitrogen base ligation occurs. We have recently reported the dynamics of the reactions of the hydroperoxide $(Ph)_2(MeOCO)COOH$ with mono

(1) Dynamics of the Reaction of [5,10,15,20-Tetrakis(2,6-dimethyl-3-sulfonatophenyl)porphinato]iron(III) Hydrate with *t*-BuOOH in Aqueous Solution. 5.

(2) Champion, P. M.; Stallard, B. R.; Wagner, G. C.; Gunsalus, I. C. *J. Am. Chem. Soc.* **1982**, *104*, 5469 and references therein.

(3) Kim, Y. O.; Goff, H. M. *Inorg. Chem.* **1990**, *29*, 3907.

(4) Castro, C. E.; Jamin, M.; Yokoyama, W.; Wade, R. *J. Am. Chem. Soc.* **1986**, *108*, 4179.

(5) Hwang, Y. C.; Dixon, D. W. *Inorg. Chem.* **1986**, *25*, 3716.

(6) Balke, V. L.; Walker, F. A.; West, J. T. *J. Am. Chem. Soc.* **1985**, *107*, 1226.

(7) Walker, F. A.; Lo, M.-W.; Ree, M. T. *J. Am. Chem. Soc.* **1976**, *98*, 5552.

(8) La Mar, G. N.; Walker, F. A. *J. Am. Chem. Soc.* **1972**, *94*, 8607.

(9) Satterlee, J. D.; La Mar, G. N.; Frye, J. S. *J. Am. Chem. Soc.* **1976**, *98*, 7276.

0002-7863/93/1515-21$04.00/0

imidazole ligated [5,10,15,20-tetrakis(2,6-dimethyl-3-sulfonatophenyl)porphinato]manganese(III) and [5,10,15,20-tetrakis(2,6-dichloro-3-sulfonatophenyl)porphinato]manganese(III) [(1)-$Mn^{III}(X)(Im)$ and (2)$Mn^{III}(X)(Im)$, respectively, where X = OH_2 and Im = imidazole + imidazolate].[10] By comparison of the kinetic parameters for these reactions with those of the aquo- or hydroxide-ligated (1)$Mn^{III}(X)(OH_2)$ and (2)$Mn^{III}(X)(OH_2)$ [X = H_2O or OH^-] at the same pH, it was shown that mono ligation by imidazole provided a 100-fold rate acceleration.[10] Our earlier studies had shown a 10-fold rate acceleration due to the effect of imidazole mono ligation on the reaction of hydrogen peroxide with (1)$Mn^{III}(X)_2$.[11]

Only qualitative estimates of the effect of nitrogen base mono ligation on the reactivity of iron(III) porphyrins with hydrogen peroxide[12] and alkyl hydroperoxides have been obtained,[13] by using a proximal nitrogen base covalently tethered to the porphyrin. This method suffers from the disadvantage that the effective concentration of the tethered base or the extent to which it ligates to the iron(III) porphyrin is not known.

Quantitative estimates of the relative reactivity of mono amine ligated complexes of iron(III) porphyrins vs uncomplexed iron(III) porphyrins toward hydroperoxides require measurements to be made under conditions which allow determination of the mole fraction of iron(III) porphyrin present as the mono nitrogen base ligated species. We report herein such a study which includes an investigation of the ligation of ammonia, trifluoroethylamine (TFEA), and imidazole to the water-soluble and non-μ-oxo-dimer-forming iron(III) porphyrin [5,10,15,20-tetrakis(2,6-dimethyl-3-sulfonatophenyl)porphinato]iron(III) [(1)$Fe^{III}(X)_2$, X = OH^- or OH_2] in aqueous solution and the influence of such ligation on the rate of reaction of iron(III) porphyrin with *t*-BuOOH. Comparison of kinetic constants from this study with those obtained in a previous study[14] performed with the analogous water-ligated complexes [(1)$Fe^{III}(X)_2$, X = OH^- or OH_2] provides the rate enhancements produced on mono ligation by the nitrogen bases.

Experimental Section

Materials. Deionized, double glass distilled water was used for all experiments. Buffer solutions were prepared from reagent grade chemicals and were passed over a chelex column. Salt solutions used to adjust ionic strengths were extracted with 0.01% dithiazone in methylene chloride to remove any heavy metal contamination. The disodium salt of 2,2'-azinobis(3-ethylbenzthiazoline-6-sulfonic acid) (ABTS) was prepared as previously described.[8] The [5,10,15,20-tetrakis(2,6-dimethyl-3-sulfonatophenyl)porphinato]iron(III) [(1)$Fe^{III}(X)_2$] was from a previous study.[15] *tert*-Butyl hydroperoxide stock solutions were prepared from 70% *t*-BuOOH in water (Aldrich). Imidazole was twice recrystallized from toluene and benzene. The other nitrogen bases were used as received.

Instrumentation. Spectrophotometric titrations and kinetic studies were conducted using either a computer-interfaced Cary-14 UV–vis spectrophotometer with On Line Instrument Systems software or Perkin-Elmer Model 553 UV–vis spectrophotometers. All spectrophotometers had cell compartments thermostated at 30 °C. pH measurements were performed with a Radiometer Model 26 pH meter using either glass or polymer bodied Corning pencil-thin electrodes. Data were analyzed using Cricket Graph software on a Macintosh II and additional software on Hewlett-Packard Model 9825A and Model 9816 computers.

Results

Complexation of (1)$Fe^{III}(X)_2$ with nitrogen bases was studied using trifluoroethylamine (TFEA) (pK_a = 5.7 at pH 5.72 and 6.8), ammonia (pK_a = 9.3 at pH 7.8 and 9.7), and imidazole (pK_a = 6.95 at pH 6.75 and 8.9). The three nitrogen bases were chosen to provide a range of base pK_a's. In a typical experiment a buffered solution containing (1)$Fe^{III}(X)_2$ [X = H_2O or HO^-] at 4×10^{-6} to 1.2×10^{-5} M was titrated with a solution of the nitrogen base in the same buffer containing the same concentration of (1)-$Fe^{III}(X)_2$. The spectral changes which take place on addition of TFEA to a solution of (1)$Fe^{III}(X)_2$ are biphasic (Figure 1). Initial addition of TFEA to final concentrations of less than 0.16 M causes an increase in absorbance at all wavelengths. Further increase in [TFEA] causes the absorbance below 399 nm to decrease, while the absorbance at higher wavelengths increases and the absorbance maximum shifts to 411 nm. The biphasic spectral changes are attributed to the initial buildup of a mono nitrogen base ligated species, followed by the formation of a bis nitrogen base ligated complex. The increase in absorbance due to formation of the bis-ligated complex was not saturable to a [TFEA] of 0.9 M. As TFEA is not soluble in H_2O at higher concentrations, we were unable to approach the saturating concentrations of TFEA and could not obtain the association constants for the binding of TFEA + (1)$Fe^{III}(H_2O)_2$ ⇌ (1)$Fe^{III}(H_2O)$-(TFEA) or TFEA + (1)$Fe^{III}(H_2O)$(TFEA) ⇌ (1)$Fe^{III}(TFEA)_2$.

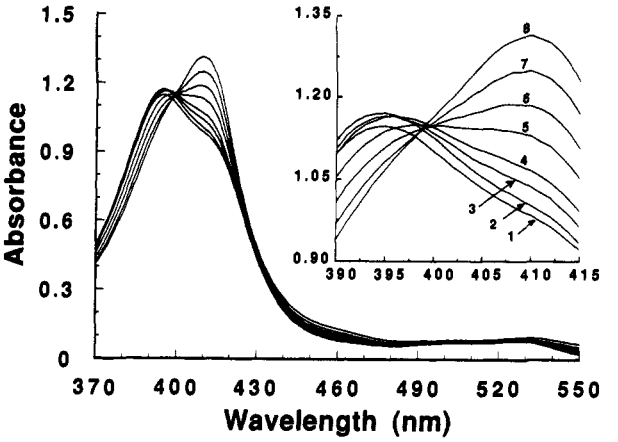

Figure 1. Spectral changes produced on ligation of $CF_3CH_2NH_2$ to the iron(III) moiety of (1)$Fe^{III}(X)_2$ (1×10^{-5} M) at pH 5.7. Concentrations of $[Am]_T$ are (starting with spectrum 1) 0, 0.163, 0.295, 0.396, 0.478, 0.605, 0.745, and 0.88 M.

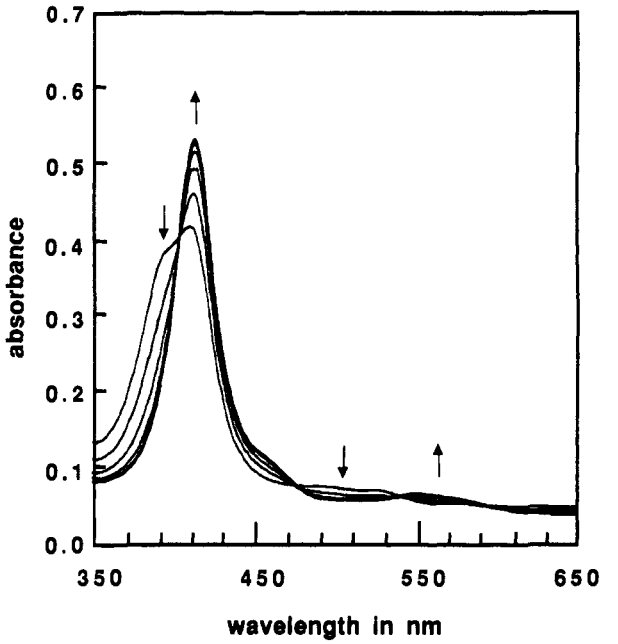

Figure 2. Changes produced in the absorption spectrum on inclusion of increasing concentrations ((0–1.9) $\times 10^{-3}$ M) of imidazole into a 3.6×10^{-6} M solution of (1)$Fe^{III}(X)_2$ at pH 6.75. Isosbestic points are at 398, 474, 537, and 594 nm.

(10) Arasasingham, R. D.; Bruice, T. C. *J. Am. Chem. Soc.* **1991**, *113*, 6095.
(11) Balasubramanian, P. N.; Schmidt, E. S.; Bruice, T. C. *J. Am. Chem. Soc.* **1987**, *109*, 7685.
(12) Robert, A.; Loock, B.; Momenteau, M.; Meunier, B. *Inorg. Chem.* **1991**, *30*, 706 and references therein.
(13) (a) Traylor, T. G.; Lee, W. A.; Stynes, D. V. *J. Am. Chem. Soc.* **1984**, *106*, 755. (b) Traylor, T. G.; Popovitz-Biro, R. *J. Am. Chem. Soc.* **1988**, *110*, 239.
(14) Gopinath, E.; Bruice, T. C. *J. Am. Chem. Soc.* **1991**, *113*, 4657.
(15) Kaaret, T. W. K.; Zhang, G. H.; Bruice, T. C. *J. Am. Chem. Soc.* **1991**, *113*, 4652.

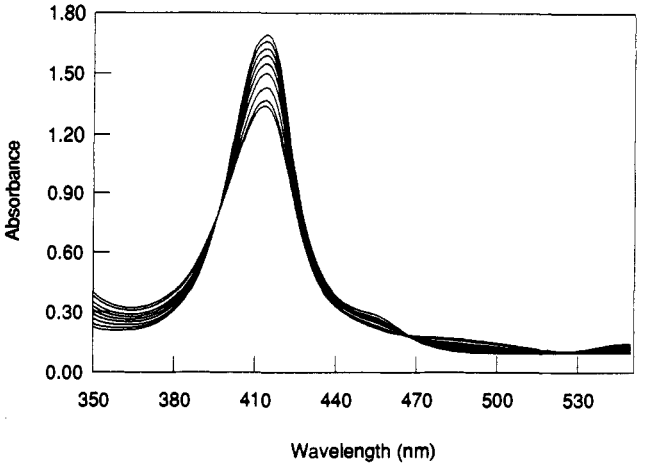

Figure 3. Changes produced in absorption spectrum on inclusion of increasing concentrations (0–1.5 M) of NH_3 into a 1.06×10^{-5} M solution of (1)$Fe^{III}(X)_2$ at pH 9.7. The λ_{max} is at 411 nm while the isosbestic points are located at 396, 467, and ~525 nm.

Scheme I

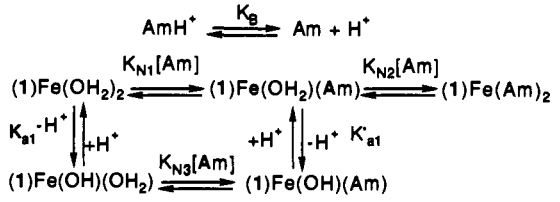

Figures 2 and 3 show the spectral changes on titration with imidazole (pH 6.74) and ammonia (pH 9.7), respectively. The changes in Figure 2 are also biphasic; no spectral change occurs at low imidazole concentrations of up to 5×10^{-5} M, while further addition of imidazole causes the shoulder at 393 nm to disappear, with an increase in absorbance at wavelengths >414 nm. In Figure 3 the initial spectrum shows a single absorption maximum at 414 nm. On addition of ammonia the spectrum gradually shifts to the final spectrum of bis ammonia ligated porphyrin with an absorption maximum at 414 nm and a shoulder at 450 nm.

In the case of ammonia and imidazole where it was possible to titrate to complete saturation in the nitrogen base, the sigmoidal plots of absorbance at 414 nm vs $[Am]_T$ have been iteratively fitted in lines generated by eq 2, which is derived from Scheme I.

$$A_{414} = \frac{(C_1 + C_2K_1[Am]_T + C_3K_2[Am]_T^2)[Fe]_T}{1 + K_1[Am]_T + K_2[Am]_T^2} \quad (2)$$

where

$$K_1 = \frac{K_B(K_{N1}a_H + K_{N3}K_{a1})}{(K_{a1} + a_H)(K_B + a_H)} \quad (3a)$$

$$K_2 = \frac{K_{N1}K_{N2}K_B^2a_H}{(K_{a1} + a_H)(K_B + a_H)^2} \quad (3b)$$

and

$$C_1 = \frac{(\epsilon_1a_H + \epsilon_2K_{a1})}{(K_{a1} + a_H)} \qquad C_2 = \frac{(\epsilon_{1N}a_H + \epsilon_{2N}K'_{a1})}{(K'_{a1} + a_H)} \quad (4)$$

$$C_3 = \epsilon_{NN}$$

where ϵ_1, ϵ_2, ϵ_{1N}, ϵ_{2N}, and ϵ_{NN} are the extinction coefficients of (1)$Fe(OH_2)_2$, (1)$Fe(OH_2)(OH)$, (1)$Fe(OH_2)(Am)$, (1)Fe(OH)(Am), and (1)$Fe(Am)_2$, respectively. Figures 4 and 5 show such plots of A_{414} vs $[NH_3]_T$ ($[NH_3]_T = [NH_3 + NH_4^+]$) (pH 7.85 and 9.7) and of A_{414} vs $[Im]_T$ ($[Im]_T$ = [imidazole + imidazole·H^+]) (pH 8.9), respectively. In eq 2, K_1 and K_2 are the pH-dependent equilibrium constants for mono and bis nitrogen base ligation to (1)$Fe^{III}(X)_2$ (eqs 3a,b), the constant C_1 is the extinction coefficient of the iron(III) porphyrin in the absence

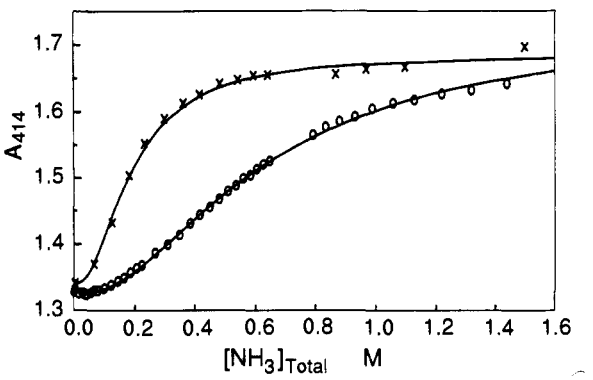

Figure 4. Plots of absorbance at 414 nm vs $[NH_3]$ for the spectrophotometric titration of (1)$Fe^{III}(X)_2$ (X = H_2O or HO^-) with NH_3 (0–1.5 M) at (i) pH 9.7 (×) and (ii) pH 7.8 (○). Studies were in H_2O at 30 °C and μ = 1.5 with $NaNO_3$. The points are experimental and the line was computer generated by iterative fitting of the points by eq 2. The values of constants that provided the lines which connect the experimental points are as follows: (i) $C_1 = 1.27 \times 10^5$ M^{-1} cm^{-1}, $C_2 = 1 \times 10^5$ M^{-1} cm^{-1}, $C_3 = 1.60 \times 10^5$ M^{-1} cm^{-1}, $K_1 = 0.2$ M^{-1}, $K_2 = 30$ M^{-2}; (ii) $C_1 = 1.27 \times 10^5$ M^{-1} cm^{-1}, $C_2 = 1 \times 10^{-5}$ M^{-1} cm^{-1}, $C_3 = 1.66 \times 10^5$ M^{-1} cm^{-1}, $K_1 = 0.26$ M^{-1}, $K_2 = 3.2$ M^{-2}.

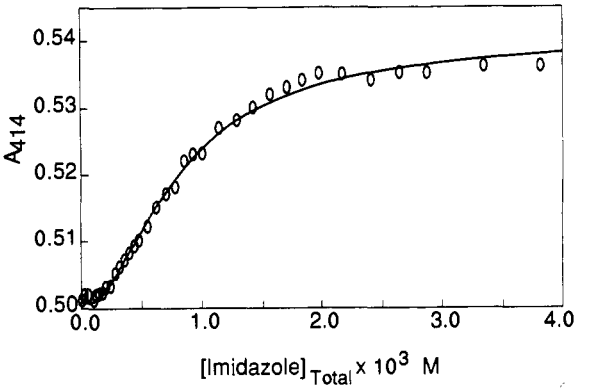

Figure 5. Plots of absorbance at 414 nm vs imidazole concentration for the spectrophotometric titration of 3.6×10^{-6} M (1)$Fe^{III}(X)_2$ (X = H_2O or HO^-) with imidazole (0–0.04 M) at pH 8.9. Studies were in H_2O at 30 °C and μ = 0.2 with $NaNO_3$. The points are experimental and the line was computer generated by iterative fitting of the points by eq 2. The values of constants employed in conjunction with eq 2 to calculate the best lines are as follows: $C_1 = 1.40 \times 10^5$ M^{-1} cm^{-1}, $C_2 = 1.33 \times 10^5$ M^{-1} cm^{-1}, $C_3 = 1.51 \times 10^5$ M^{-1} cm^{-1}, $K_1 = 319$ M^{-1}, $K_2 = 2.16 \times 10^6$ M^{-2}.

of nitrogen base and at a given pH [i.e., it is the sum of the extinctions multiplied by the mole fractions of (1)$Fe^{III}(OH_2)_2$ and (1)$Fe^{III}(OH)(OH_2)$ at a given pH (eq 4)], and C_2 is the extinction coefficient of the iron(III) porphyrin ligated to one nitrogen base [i.e., it is the sum of the extinction (ϵ_{1N}) multiplied by the mole fraction of (1)$Fe^{III}(OH_2)(Am)$ and the extinction (ϵ_{2N}) multiplied by the mole fraction of (1)$Fe^{III}(OH)(Am)$ at a given pH (eq 4)], while C_3 is simply the extinction coefficient (ϵ_{NN}) for (1)-$Fe^{III}(Am)_2$. The deviation of eq 2 assumes sequential mono and bis ligation of nitrogen base to (1)$Fe^{III}(OH_2)_2$ but only mono ligation of nitrogen base to (1)$Fe^{III}(OH)(OH_2)$ (Scheme I). In practice, the extinction coefficients of ϵ_{1N} for (1)$Fe^{III}(OH_2)(Am)$ and ϵ_{2N} for (1)$Fe^{III}(OH)(Am)$ cannot be determined since one cannot saturate the iron(III) porphyrin with 1 equiv of nitrogen base without the formation of the bis nitrogen base ligated product. Therefore, the dependence of A_{414} on $[Am]_T$ was fit to eq 2 using several assumed C_2 values ranging from 500 to 1.3×10^5 M^{-1} cm^{-1}. By this means, a set of values of K_1 and K_2 corresponding to the set of assumed C_2 values was obtained at each pH. From two sets of "n" K_1 values obtained at two pH values, ($n \times n$) possible pairs of K_1 values at the two pH's were obtained. Each pair of K_1 values, when substituted into eq 3a, provides a set of two equations which are then solved to provide values for the pH-independent constants K_{N1} and K_{N3} (Scheme I). This process

Table I. Equilibrium Constants for Mono and Bis Ligation of Ammonia and Imidazole to (1)$Fe^{III}(OH_2)_2$ (K_{N1} and K_{N2}) and (1)$Fe^{III}(OH)(OH_2)$ (K_{N3}) Obtained from the Solution of Equation 3

	ligation of	
equilibrium constants	ammonia	imidazole
K_{N1} (M^{-1})	$(0.1–1.5) \times 10^2$	$(1–5) \times 10^3$
K_{N2} (M^{-1})	$(0.3–6) \times 10^3$	$(0.3–3.2) \times 10^5$
K_{N3} (M^{-1})	0.6–0.9	0.9–900
$K_{N1}K_{N2}$ (β) (M^{-2})	$(4.4–8.4) \times 10^4$	$(5–8) \times 10^8$

enabled calculation of the range of K_{N1} and K_{N3} values that is possible.

For example, plots of A_{414} vs $[NH_3]_T$ could be fit to eq 2 with C_2 values ranging from 500 to 130 000 M^{-1} cm^{-1} (C_1 = 128 300 M^{-1} cm^{-1}). Eighteen values of K_1 were calculated at each pH by varying C_2 values over this range. These K_1 values ranged from 0.05 to 0.5 M^{-1} at pH 7.85 and from 0.04 to 0.4 M^{-1} at pH 9.7. The solution of eq 3a with all possible combinations of these values provided K_{N1} values ranging from 10 to 20 M^{-1} if C_2 = 500 M^{-1} cm^{-1}, which increased to 100–150 M^{-1} if C_2 = 115 000 M^{-1} cm^{-1}. If C_2 values are a lot smaller than corresponding values of C_1, then the ligation of ammonia by iron(III) porphyrin must produce a dramatic and unprecedented quenching of the soret absorbance. Thus we favor the higher values for K_{N1} as being more plausible. K_{N3} values obtained thus showed less variation (0.65 ± 0.2 M^{-1}) with C_2 values from 500 to 90 000 M^{-1} cm^{-1}, but they drop down to 0.155 M^{-1} when C_2 values are increased from 90 000 to 100 000 M^{-1} cm^{-1}. With C_2 > 105 000 M^{-1} cm^{-1}, negative values of K_{N3} result. Since K_{N3} cannot be negative, C_2 < 105 000 M^{-1} cm^{-1}. K_2 values at a fixed pH show little variation with C_2, as do the values of β ($\beta = K_{N1}K_{N2}$), obtained by solving eq 3b with the K_2 values obtained at either pH value (Table I). Analysis of plots of A_{414} vs $[Im]_T$ obtained at pH 6.75 and 8.9 in the same manner produces the range of values for K_{N1}, K_{N3}, and $K_{N1}K_{N2}$ provided in Table I. Inspection of Table I shows that K_{N1}, K_{N3}, and $K_{N1}K_{N2}$ for ligation of imidazole are all higher than those for ligation of NH_3. The corresponding equilibrium constants for ligation of TFEA are qualitatively estimated to be lower than those for NH_3, but a more quantitative comparison is not possible.

Kinetic Studies. The influence of ligation by nitrogen base to provide (1)$Fe^{III}(OH_2)$(Am) and (1)Fe^{III}(OH)(Am) on the dynamics of reactions of the iron(III) porphyrin with *t*-BuOOH was investigated using disodium 2,2′-azinobis(3-ethylbenzthiazoline-sulfonate) (ABTS) as a one-electron oxidizable trap for products which are oxidants (30 °C and μ = 0.2). The one-electron oxidation of ABTS provides $ABTS^{\bullet+}$, which may be followed at 660 nm. Typically, reactions were carried out in buffered, aerobic, aqueous solution with [(1)Fe^{III}(X)(Y)] < [*t*-BuOOH]$_i$ < [ABTS] < $[Am]_T$. The *t*-BuOOH was in 10–80-fold excess over (1)-Fe^{III}(X)(Am) catalyst (X = H_2O or HO^-). The concentration of ABTS was maintained at 5×10^{-3} M, and the concentration of nitrogen base varied over $(0–6) \times 10^{-2}$ M. The pK_a for the ionization of (1)$Fe^{III}(OH_2)_2 \rightarrow$ (1)$Fe^{III}(OH_2)(OH^-) + H^+$ is at pH 6.7.[14]

With trifluoroethylamine (TFEA), two sets of reactions were performed. In the first, the concentration of (1)Fe^{III}(X)(Y) was varied [7.3×10^{-7} to 8.6×10^{-6} M] and $[TFEA]_T$ ($[TFEA]_T$ = [TFEA] + [TFEA·H^+]) was maintained constant at ~50 mM. In the second set of reactions, $[TFEA]_T$ was varied (0–50 mM) and the concentration of (1)$Fe^{III}(X)_2$ was maintained constant (~7×10^{-6} M). All reactions followed the first-order rate law to >95% completion at all concentrations of iron(III) porphyrin and TFEA employed. Both sets of experiments were performed at seven different pH values ranging from 4.5 to 7.4. Buffers used were CH_3COO^-/CH_3COOH (pH 4.5–5.3) and $H_2PO_4^-/HPO_4^{2-}$ (pH 5.3–7.4). When iron(III) porphyrin was varied and $[TFEA]_T$ was kept constant at 5×10^{-2} M, plots of the observed first-order rate constants (k_{obsd}) vs [(1)$Fe^{III}(X)_2$] were linear and passed through the origin (Figure 6). This shows the reaction to be first order in iron(III) porphyrin and *t*-BuOOH with no uncatalyzed decomposition of hydroperoxide. Therefore, in experiments where the concentration of iron(III) porphyrin was kept constant and

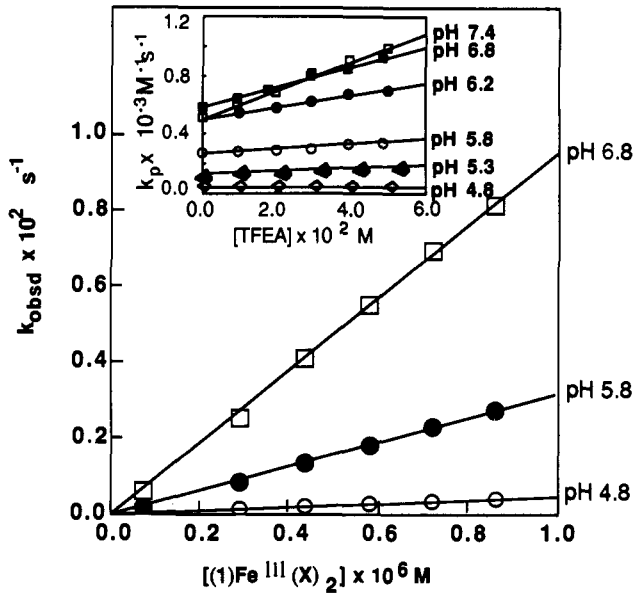

Figure 6. Plots showing the linear dependence of the first-order rate constants for the (1)$Fe^{III}(X)_2$ catalyzed reduction of *t*-BuOOH (k_{obsd}) on (1)$Fe^{III}(X)_2$, in the presence of $CF_3CH_2NH_2$ (TFEA) at 30 °C and μ = 0.2. In each of these experiments, $[TFEA]_T$ = [TFEA + TFEA·H^+] was held constant at 5×10^{-2} M and the pH was at the values indicated. Inset: Plots showing the linear dependence of the second-order rate constants (k_p) on $[TFEA]_T$ for the iron(III) porphyrin catalyzed reduction of *t*-BuOOH. Experiments were carried out at 30 °C and μ = 0.2 with the pH held constant at the values indicated alongside the corresponding plot.

$[TFEA]_T$ was varied, values of the apparent second-order rate constants (k_p) were obtained by simply dividing k_{obsd} by the total concentration of iron(III) porphyrin (eq 5). These k_p values are

$$-d[t\text{-BuOOH}]/dt = k_{obsd}[t\text{-BuOOH}] \quad (5a)$$

$$k_{obsd} = k_p[(1)Fe^{III}(X)_2] \quad (5b)$$

$$k_p = k_{BT}[TFEA]_T + k_{ly} \quad (5c)$$

a composite of the pH-dependent second-order rate constants (k_{ly}) for the reaction of *t*-BuOOH with (1)$Fe^{III}(H_2O)_2$ and (1)Fe^{III}-(OH)(H_2O), as well as the pH-dependent third-order rate constants (k_{BT}) for reaction of (1)$Fe^{III}(H_2O)$(TFEA) and (1)Fe^{III}-(OH)(TFEA) at a given pH and TFEA concentration (eq 5). The slopes of plots of k_p vs $[TFEA]_T$ (Figure 6, inset) provided the pH-dependent third-order rate constants for the nitrogen base catalyzed reaction (k_{BT}), and the intercepts yielded the pH-dependent and nitrogen base independent second-order rate constant (k_{ly}). The k_{ly} values obtained in this manner are numerically the same as those previously reported[14] from extensive experiments carried out in the absence of nitrogen base. This finding confirms that the k_{obsd} vs $[TFEA]_T$ plots remain linear at $[TFEA]_T$ approaching zero. Attempts to introduce nonlinearity into the TFEA dilution plots by saturating the porphyrin with TFEA were unsuccessful, due to precipitation of reactants from solution at high TFEA concentration. Values of k_{BT} (eq 5) were determined at several pH values over the pH range 3–7. The dependence of k_{BT} values on pH is shown in Figure 7. The points are experimental and the line was generated by iterative fitting of the points to eq 6. Equation 6 follows from the reaction sequences of Scheme II (see the Appendix).

$$k_{BT} = \frac{\frac{k'_1k'_2}{(k'_2 + k'_{-1})}K_{N1}K_Ba_H\left\{a_H + \frac{k'_4}{k'_2}K'_{a3}\right\}}{(K_{a1} + a_H)(K_B + a_H)\left\{a_H + \frac{k'_4}{(k'_2 + k'_{-1})}K'_{a3}\right\}} \quad (6)$$

The effect of ammonia on the kinetics of the reaction of the iron(III) porphyrin with *t*-BuOOH was examined over a range

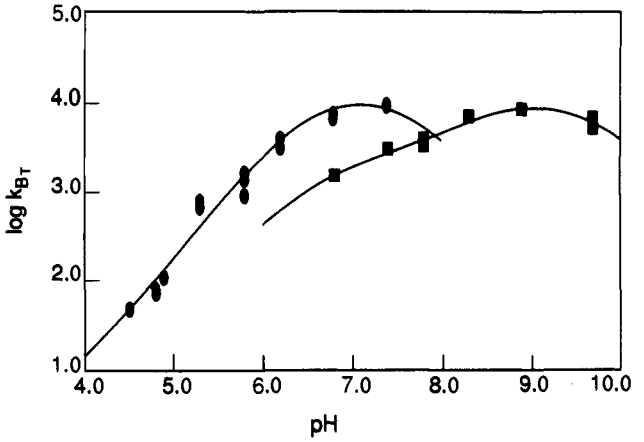

Figure 7. pH dependence of the third-order rate constants (k_{BT}) for the reduction of *t*-BuOOH by (1)$Fe^{III}(X)_2$ catalyzed by (●) $[TFEA]_T$ and (■) $[NH_3]_T$. The points are experimental and the line was generated by iterative fitting of points to eq 6. The kinetic constants used to generate the line shown are in Table II.

Scheme II

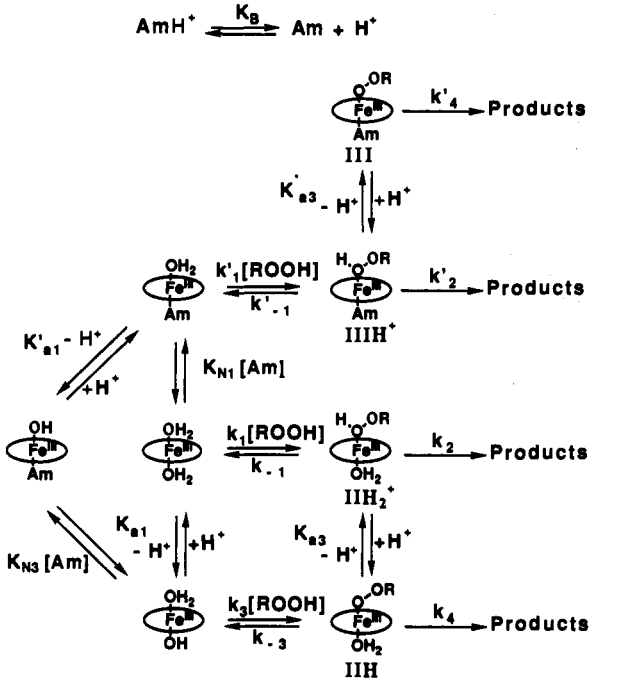

of low and high concentrations of $[NH_3]_T$ ($[NH_3]_T = [NH_3] + [NH_4^+]$). The dependence of the rate constants on $[NH_3]_T$ is different at high and low concentrations of $[NH_3]_T$.

At the low range of $[NH_3]_T$, a series of experiments was performed in which the initial concentration of (1)$Fe^{III}(X)_2$ varied from 4×10^{-7} to 7×10^{-6} M for each experiment and the $[NH_3]_T$ was held constant. The experiments were performed over at least a 5-fold range of $[NH_3]_T$ at each pH. The plots of k_{obsd} vs [(1)$Fe^{III}(X)_2$] were linear at all pH values and exhibited small intercepts at ≥pH 9. Figure 8 shows such a series of experiments at pH 8.9. The slopes of the plots are equal to k_p (eq 7). The

$$-d[t\text{-BuOOH}]/dt = k_{obsd}[t\text{-BuOOH}] \quad (7a)$$

$$k_{obsd} = \{k_{BT}[NH_3]_T + k_{ly}\}[(1)Fe^{III}(X)_2] + k_o \quad (7b)$$

$$k_p = \{k_{BT}[NH_3]_T + k_{ly}\} \quad (7c)$$

slopes of the secondary plots (Figure 9A) of k_p vs $[NH_3]_T$ provide the apparent third-order rate constants (k_{BT}), and the intercepts equal the pH-dependent second-order rate constants (k_{ly}) for reaction of the iron(III) porphyrin with *t*-BuOOH. Values of k_{ly} so determined are the same (within experimental error) as those previously obtained in the absence of ammonia.[14] This shows that

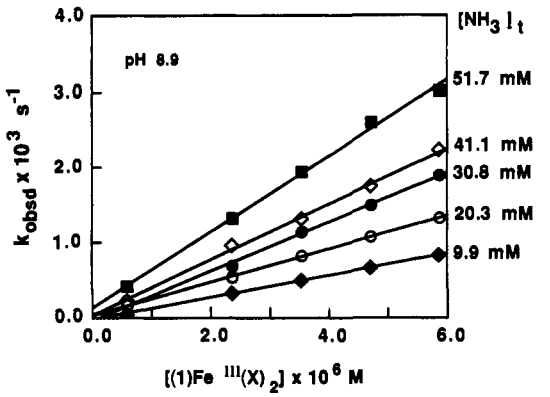

Figure 8. Plots showing the linear dependence of the first-order rate constants for the decomposition of *t*-BuOOH (k_{obsd}) on the initial concentration of iron(III) porphyrin catalyst in the presence of NH_3, at pH 8.9, 30 °C, and $\mu = 0.2$. In each of these experiments, $[NH_3 + NH_4^+]$ was held constant at the values indicated in the right-hand margin.

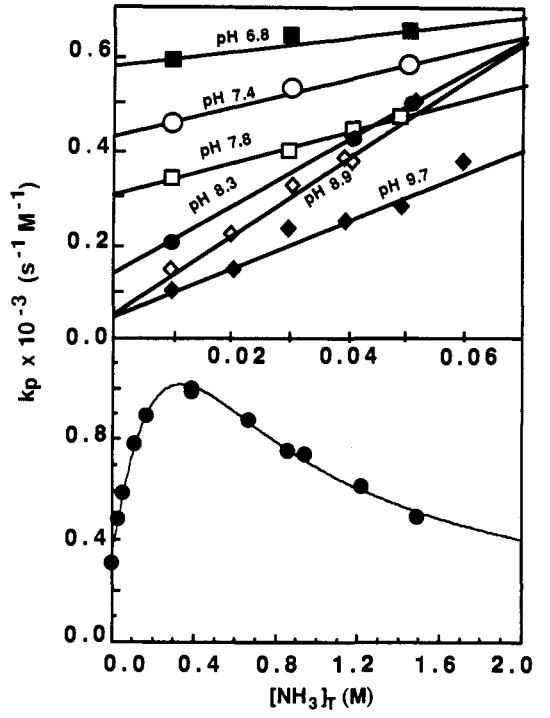

Figure 9. Dependence of the second-order rate constants (k_p) for the iron(III) porphyrin catalyzed reduction of *t*-BuOOH on $[NH_3]_T$ ($[NH_3]_T = [NH_3 + NH_4^+]$) present. Experiments were carried out at 30 °C and $\mu = 0.2$. (A, top) Plots of k_p vs $[NH_3]_t$ at the lowest concentrations of the latter are linear. The pH was held constant at the values indicated along the lines. (B, bottom) Plot of k_p vs $[NH_3]_t$ at higher concentrations of the latter (pH 7.8, 30 °C, and $\mu = 1.5$). The points are experimental, and the line was generated by iterative fitting of the points to eq 7. The kinetic constants used to generate the line shown are as follows: $k_{ly} = 3.2 \times 10^2\ M^{-1}\ s^{-1}$; $k_{BT} = 3.2 \times 10^3\ M^{-2}\ s^{-1}$, $K_1 = 1.3\ M^{-1}$, and $K_2 = 6.1\ M^{-2}$.

eq 7b is followed over this entire range of $[NH_3]_T$. Values of k_{BT} were determined between pH 6.8 and 9.7. Above pH 9.7 the experiments were complicated, presumably due to loss of ammonia gas from solution. A plot showing the dependence of k_{BT} on pH is shown in Figure 7. The points are experimental and the line is generated by iterative fitting of the points to eq 6, which is derived from Scheme II with the assumption that in this range of $[NH_3]_T$ the ammonia-ligated porphyrin species represent a small fraction of the total [(1)$Fe^{III}(X)_2$]. Values of rate and equilibrium constants obtained from fitting the two sets of experimental points in Figure 7 by eq 6 are provided in Table II. The kinetic constants for the reaction of [(1)$Fe^{III}(X)_2$] with *t*-BuOOH in the absence of nitrogen base were determined in a previous study[14] to be $k_1k_2/(k_2 + k_{-1}) = 5.0\ M^{-1}\ s^{-1}$, $(k_4/k_2)K_{a3} = 1.4 \times 10^{-4}$ M, (k_4

Table II. Values of Rate and Equilibrium Constants Obtained by Fitting Equation 6 to the Two Sets of Experimental Points in Figure 7

kinetic terms[a]	values of determined constants in reaction of (1)$Fe^{III}(X)_2$ with $(Me)_3COOH$ catalyzed by ammonia	trifluoroethylamine
$k'_1k'_2(k'_2 + k'_{-1})K_{N1}$	1.1×10^6	0.7×10^3
$(k'_4/k'_2)K'_{a3}$	1.1×10^{-8}	5.7×10^{-6}
$k'_4K'_{a3}/(k'_2 + k'_{-1})$	1.4×10^{-9}	4.2×10^{-8}
K_{a1}	1.8×10^{-7}	1.8×10^{-7}
K_B	4.5×10^{-10}	2.0×10^{-6}

[a] Units in moles, seconds.

$+ k_{-3})K_{a3}/(k_2 + k_{-1}) = 5.5 \times 10^{-7}$.

At higher $[NH_3]_T$ the order of the dependence of k_p on $[NH_3]_T$ decreases from 1 to 0 and finally to −1, such that eq 7c no longer pertains (Figure 9B). The experimental points in Figure 9B are $k_{obsd}/[(1)Fe^{III}(X)_2] = k_p$ at $[NH_3]_T$ varying from 0 to 1.5 M, pH 7.85 and $\mu = 1.5$. The curve has been generated by iterative fitting of the points to eq 8, which is derived from Scheme II (see the Appendix for derivation) with the assumption that in this range of $[NH_3]_T$ ammonia-ligated porphyrin species represent a large fraction of the total iron(III) porphyrin used. Fitting of the experimental points of Figure 9B to eq 8 provides the following values: $k_{ly} = 320\ M^{-1}\ s^{-1}$; $k_{BT} = 3225\ M^{-2}\ s^{-1}$; $K_1 = 1.3\ M^{-1}$; $K_2 = 6.1\ M^{-2}$.

$$k_{obsd} = k_p[(1)Fe^{III}(X)_2] = \frac{(k_{ly} + k_{BT}[Am]_T)[(1)Fe^{III}(X)_2]}{1 + K_1[Am]_T + K_2[Am]_T^2} \quad (8)$$

The effect of imidazole concentration on the kinetics of the reaction of the iron(III) porphyrin with *t*-BuOOH was determined spectrophotometrically as described for reactions in the presence of NH_3 and TFEA. All reactions followed the first-order rate law to completion. First-order rate constants (k_{obsd}) were obtained at $[Im]_T$ ($[Im]_T$ = [imidazole] + [imidazole·H^+]) ranging from 0 to 0.015 M with $[(1)Fe^{III}(X)_2]$ at 8×10^{-6} M at pH 6.8 and 7.4. The values of k_{obsd} so obtained first decreased with increasing $[Im]_T$ and then leveled off at higher $[Im]_T$. In Figure 10 the points are experimental and the line is generated by iterative fitting of the points to eq 8, which is derived from Scheme II (see the Appendix for derivation). The optimum values of constants required for the fitting of the experimental data to eq 8 are as follows: $k_{ly} = 6.3 \times 10^2\ M^{-1}\ s^{-1}$; $k_{BT} = 1.1 \times 10^6\ M^{-2}\ s^{-1}$; $K_1 = 2.3 \times 10^3\ M^{-1}$; $K_2 = 6.0 \times 10^7\ M^{-2}$.

Hydroxylamine is not formed in the reaction of *t*-BuOOH with the iron(III) porphyrin in ammonia. This was determined by examining the effect of hydroxylamine on the reaction of the iron(III) porphyrin with *t*-BuOOH. Under conditions of $[(1)Fe^{III}(X)_2] = 6.68 \times 10^{-6}$ M, pH 6.2, and $[NH_2OH] = 10$, 20, 30, 40, and 50 mM, the $ABTS^{\bullet+}$ radical was not observed. Independent experiments showed that this was due to the reduction of $ABTS^{\bullet+}$ by NH_2OH. Thus addition of NH_2OH or NH_2OCH_3 to a spent reaction solution which initially contained *t*-BuOOH + (1)$Fe^{III}(X)_2$ + ABTS resulted in the bleaching of the $ABTS^{\bullet+}$ product within 5 min. The stoichiometry of this reduction was determined by varying $[NH_2OH]$ at stoichiometric levels relative to *t*-BuOOH ($[(1)Fe^{III}(X)_2] = \sim 8 \times 10^{-6}$ M, [*t*-BuOOH] = $\sim 5 \times 10^{-5}$ M, $[NH_2OH] = (0, 1, 3, 6, 10, 15) \times 10^{-5}$ M, pH 6.2). $ABTS^{\bullet+}$ yields varied linearly with the amount of hydroxylamine added, such that 1.5–1.6 equiv of $ABTS^{\bullet+}$ were bleached per equivalent of hydroxylamine. Thus hydroxylamine is not formed in the ammonia-catalyzed reaction of *t*-BuOOH with the iron(III) porphyrin, since in the latter experiments stoichiometric yields of $ATBS^{\bullet+}$ were obtained.

Discussion

Ligation of TFEA, Imidazole, and NH_3 by (1)$Fe^{III}(X)(OH_2)$ (where X = OH^- or OH_2). The dependence of the UV–vis spectra of the iron(III) porphyrin on the concentration of added nitrogen base provided evidence for the accumulation of a mono-ligated

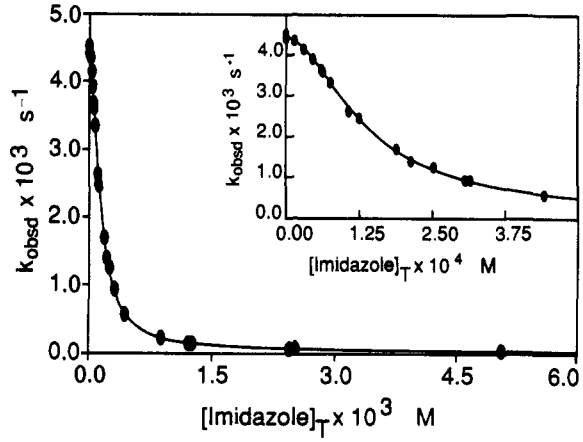

Figure 10. Plot showing the dependence of the first-order rate constants for the iron(III) porphyrin catalyzed reduction of *t*-BuOOH (k_{obsd}) on the total concentration of imidazole $[Im]_T$ ($[Im]_T$ = [imidazole + imidazole-H^+]), at pH 6.8, 30 °C, and $\mu = 0.2$. The points are experimental, and the line was generated by iterative fitting of the points to eq 7. The kinetic constants used to generate the line shown are as follows: $k_{ly} = 6.3 \times 10^2\ M^{-1}\ s^{-1}$, $k_{BT} = 1.1 \times 10^6\ M^{-2}\ s^{-1}$, $K_1 = 2.3 \times 10^3\ M^{-1}$, and $K_2 = 6.0 \times 10^7\ M^{-2}$.

complex prior to bis ligation. This is most readily apparent on inspection of Figure 1, which shows the absorbance changes produced on the addition of trifluoroethylamine at pH 5.7. At this pH the initial spectrum is of (1)$Fe^{III}(OH_2)_2$ and shows a maximum at 393 nm with a shoulder at 411 nm. Initial addition of TFEA causes the absorbance at 393 nm to be enhanced due to formation of (1)Fe^{III}(TFEA)(OH_2); with further addition of TFEA the absorbance at 393 nm drops, and the maximum absorbance shifts to the 411-nm maximum characteristic of the bis nitrogen base ligated complexes. Ammonia and imidazole, having higher pK_a's were examined at higher pH's where the initial spectrum is dominated by the absorbance due to (1)Fe^{III}(OH)-(OH_2) (maximum at 411 nm). Thus, here the only spectral change is an increase in the absorbance intensity at 411 nm on addition of nitrogen base (see Figures 2 and 3). This increase is biphasic, and the increase in absorbance at 414 nm displays a sigmoidal dependence upon $[Am]_T$ (Figures 4 and 5). The change in A_{414} accompanying the titration of (1)$Fe^{III}(X)_2$ with ammonia or imidazole followed an equation (eq 2) derived with the assumption of sequential mono and bis ligation of nitrogen base to (1)-$Fe^{III}(OH_2)_2$ but only mono ligation to (1)$Fe^{III}(OH)(OH_2)$ (Scheme I). The extinction coefficients of the nitrogen base mono-ligated species (1)$Fe^{III}(Am)(OH_2)$ and (1)$Fe^{III}(Am)(OH)$ at 414 nm are unknown, but must be assumed to be approximately equal to or below that of (1)$Fe^{III}(OH_2)_2$ or (1)$Fe^{III}(OH)(OH_2)$ at a given pH in order to fit the experimental data to eq 2. The extinction coefficients of the mono nitrogen base ligated species at 414 nm were arbitrarily assumed to be between 500 and 130000 $M^{-1}\ s^{-1}$, and a range of possible values were calculated for each equilibrium constant (Table I). Owing to the lower affinity of (1)$Fe^{III}(X)(OH_2)$ for TFEA and the latter's limited solubility in water, it was not possible to determine equilibrium constants for mono and bis ligation of this nitrogen base.

Numerous prior investigations of the ligation of imidazole to different porphyrins in various solvents have been carried out.[6-9] However, most of these studies have concentrated on the determination of the equilibrium constant for ligation of two molecules of nitrogen base to $[(por)Fe^{III}]^+$ to form the low-spin, bis nitrogen base ligated species $(por)Fe^{III}(Am)_2$, and the mono-ligated species were generally not observed (NMR or UV–vis spectra). Walker et al. have reported spectral evidence to support the presence of mono-ligated species using "sterically demanding"[8] 2-methylimidazole or *N*-methylimidazole at low ratios of nitrogen base to iron(III) porphyrin. In these cases the data were analyzed with the assumption that the spectral change on adding the first amine ligand was of the same magnitude and direction as the spectral change produced on ligation of a second molecule of amine.

Although the assumption concerning extinction coefficients is not correct, the binding constants calculated by this method for the mono ligation of *N*-methylimidazole to various substituted tetraphenylporphyrins (12–80 M^{-1} in $CHCl_3$)[8] are close to the K_1 values of a recent study on the ligation of *N*-methylimidazole to a capped porphyrin (in $CHCl_3$), in which only mono ligation can occur.[16]

In our system, mono ligation was observable on titration with each of the three nitorgen bases (Scheme I). The equilibrium constant (K_{N1}) determined in water for ligation of imidazole with (1)$Fe^{III}(H_2O)_2$ ((1–5) × 10^3 M^{-1}, Table I) and the product of the equilibrium constants for mono and bis ligation ($\beta = K_{N1}K_{N2}$) of imidazole ((5–8) × 10^8 M^{-2}) were each ~2 orders of magnitude greater than the values reported by Walker et al.[7,8] for mono and bis ligation of *N*-methylimidazole to (TPP)Fe^{III}(Cl) in $CHCl_3$, respectively. K_{N1} values determined by us for the ligation of ammonia to (1)$Fe^{III}(OH_2)_2$ (10–150 M^{-1}) are 1–2 orders of magnitude smaller than those which we found for the ligation of imidazole. However, values of β ((4.4–8.4) × 10^4 M^{-2}) obtained for bis ligation by ammonia were ~4 orders of magnitude smaller than corresponding values for bis ligation of imidazole. Thus, a much larger fraction of iron(III) porphyrin can exist as the mononitrogen base ligated species at a given concentration of ammonia than at corresponding concentrations of imidazole. On titration of (1)$Fe^{III}(OH_2)_2$ with TFEA, it was not possible to achieve saturation in TFEA. At TFEA concentrations of 0.9 M, plots of A_{414} vs $[TFEA]_T$ are still linear, indicating that the complexation of $[TFEA]_T$ to iron(III) porphyrin is <30% complete. At equivalent concentrations of ammonia, formation of the bis ammonia complex is essentially complete. Therefore, β values for TFEA are likely to be at least 1 order of magnitude smaller than with ammonia.

Influence of Nitrogen Base Ligation of [(1)$Fe^{III}(H_2O)$] and [(1)Fe^{III}(OH)] on the Dynamics of the Reactions of the Iron(III) Porphyrin with *t*-BuOOH (30 °C and μ = 0.2). The reaction of *t*-BuOOH with iron(III) porphyrin in the presence of nitrogen base results from competing reactions characterized by the pH-dependent expressions $k_{1y}[t\text{-BuOOH}][(1)Fe^{III}(X)_2]$ and $k_{BT}[t\text{-BuOOH}][(1)Fe^{III}(X)(Am)]$ where X = H_2O or HO^-. The constant k_p is defined as $k_p = k_{BT}[Am]_T + k_{1y}$. The dependence of k_p values on the concentration of nitrogen base is linear at all concentrations of the weakly ligating TFEA and at low concentrations (0–0.06 M) of the more strongly ligating ammonia (eqs 5 and 7, respectively). At higher concentrations of ammonia and at all concentrations of imidazole, the dependence of k_p on nitrogen base follows eq 8. The linear increase in k_p with an increase in the concentration of nitrogen base (at low nitrogen base concentration) is attributed to the formation of (1)Fe^{III}(Am)(H_2O), which is more reactive than (1)$Fe^{III}(H_2O)_2$ or (1)Fe^{III}(OH)(H_2O) [the complex (1)Fe^{III}(Am)(OH) is unreactive].

At the concentrations of ammonia and TFEA used, the mono nitrogen base ligated iron(III) porphyrin species are present in concentrations that are sufficiently small to ignore in the material balance calculation (eq 7), but are kinetically significant and must appear in the rate terms. Third-order rate constants (k_{BT}) for the reaction of the iron(III) porphyrin with *t*-BuOOH catalyzed by ammonia and TFEA were obtained from the slopes of linear plots of k_p vs $[Am]_T$. The constants k_{BT} exhibit a pH dependence (Figure 7) which is correlated by eq 6 which, in turn, is derived from the reaction sequences of Scheme II. Although the same equation (eq 6) is used to fit the log k_{BT} vs pH plots for both TFEA and NH_3 (Figure 7), the shapes of the curves generated are distinctly different and reflect the different pK_a's of NH_4^+ and $CF_3CH_2NH_2{\cdot}H^+$ and the different mole fractions of iron(III) porphyrin present as (1)$Fe^{III}(OH_2)_2$ in the different pH regions. The maximum values of k_{BT} obtained with NH_3 and TFEA are almost identical. Although the rate enhancement produced by ligation of NH_3 to (1)$Fe^{III}(OH_2)_2$ is greater than that produced on ligation of TFEA, in the pH range where a large fraction of $[NH_3]_T$ is present as NH_3 very little (1)$Fe^{III}(X)_2$ is present as (1)$Fe^{III}(OH_2)_2$ and vice versa. This is not the case with TFEA at pH values between 5 and 7, where substantial mole fractions of both $[TFEA]_T$ and (1)$Fe^{III}(X)_2$ are present as the dissociated TFEA and the undissociated (1)$Fe^{III}(OH_2)_2$.

The kinetic constants used in the fitting of eq 6 to the pH dependence of k_{BT} are provided in Table II. The kinetic term $k'_1k'_2/(k'_2 + k'_{-1})K_{N1}$ is the third-order rate constant for nitrogen base catalysis of the reaction of (1)$Fe^{III}(OH_2)_2$ with *t*-BuOOH. The value of this term is seen to be 10^3-fold higher with ammonia than with TFEA. Division of this term by the association constant for ligation of nitrogen base to (1)$Fe^{III}(OH_2)_2$ to form (1)Fe^{III}-(OH_2)(Am) (i.e., K_{N1}) provides the rate constant $k'_1k'_2/(k'_2 + k'_{-1})$ for reaction of (1)$Fe^{III}(OH_2)$(Am) + *t*-BuOOH (eq 9).

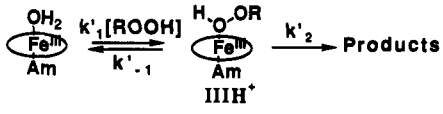

(9)

When Am = NH_3, $k'_1k'_2/(k'_2 + k'_{-1})K_{N1}$ = 1.1 × 10^6 M^{-2} s^{-1}. At the highest possible value of K_{N1} [= 150 M^{-1} (Table I)], the overall second-order rate constant $[k'_1k'_2/(k'_2 + k'_{-1})]$ for the reaction of eq 9 equals 7.3 × 10^3 M^{-1} s^{-1}. The rate constant $[k_1k_2/(k_2 + k_{-1})]$ for the reaction of (1)$Fe^{III}(OH_2)_2$ + *t*-BuOOH (eq 10) has been determined in a previous study[14] to be 5.0 M^{-1} s^{-1}.

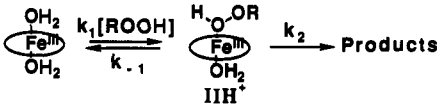

(10)

On the basis of the K_{N1} value employed, the ratio of the second-order rate constants for the reactions of (1)$Fe^{III}(OH_2)$(NH_3) and (1)$Fe^{III}(OH_2)_2$ with *t*-BuOOH is 1.4 × 10^3. This is the *minimal* rate enhancement brought about by NH_3 ligation. If the value of K_{N1} were to be at the low end of the calculated range (Table I), the rate enhancement would be 10^5-fold. Comparison of the minimal rate enhancement produced on ligation of NH_3 to (1)$Fe^{III}(OH_2)_2$ to form (1)$Fe^{III}(OH_2)(NH_3)$ (10^3–10^5-fold) with the rate enhancement produced on ionization of (1)$Fe^{III}(OH_2)_2$ to (1)$Fe^{III}(OH_2)$(OH) (1.1 × 10^2)[22b] shows that a 10–1000-fold greater rate enhancement is realized on substitution of H_2O by NH_3 rather than by OH^-. When Am = TFEA, the term $k'_1k'_2/(k'_2 + k'_{-1})K_{N1}$ was determined to be 7.0 × 10^2 M^{-2} s^{-1}. However, similar calculation of the rate enhancement produced on ligation of TFEA was precluded by our inability to determine K_{N1} for TFEA ligation to (1)$Fe^{III}(OH_2)_2$. Comparison of this third-order rate constant with the second-order rate constant (5.0 M^{-1} s^{-1}) for reaction of (1)$Fe^{III}(OH_2)_2$ + *t*-BuOOH (eq 10) provides $[k'_1k'_2/(k'_2 + k'_{-1})K_{N1}]/[k_1k_2/(k_2 + k_{-1})]$ = 1.4 × 10^2 M^{-1}. This number represents K_{N1} multiplied by the rate enhancement to be produced on ligation of TFEA. Thus if K_{N1} were to be >140 M^{-1}, no rate enhancement would accompany ligation of TFEA. However, the affinity of TFEA for (1)$Fe^{III}(OH_2)_2$ is seen to be much lower than that of NH_3, so that K_{N1} is very likely to be much lower than this value.

At higher concentrations, NH_3 becomes inhibitory rather than catalytic (Figure 9B). This attenuation results from an increasing proportion of the iron porphyrin catalyst being sequestered in a bis NH_3 ligated complex [(1)$Fe^{III}(NH_3)_2$] which does not ligate *t*-BuOOH. Above $[NH_3]_T$ > 0.06 M, the concentration of (1)-$Fe^{III}(NH_3)_2$ does represent a significant mole fraction of total iron(III) porphyrin such that the concentration of (1)$Fe^{III}(NH_3)_2$ must be taken into account in the material balance equation. Thus, the dependence of the k_{obsd} values upon $[NH_3]_T$ is described by eq 8. From fitting the kinetic data to eq 8, the pH-dependent equilibrium constants for mono and bis ligation at pH 7.85 (K_1 = 0.05–0.5 M^{-1} and K_2 = 3.0–3.3 M^{-2}, respectively) are in reasonable agreement with thermodynamic ligation constants determined at the same pH (K_1 = 0.3–2.0 M^{-1} and K_2 = 5–7 M^{-2}).

The equilibrium constant for mono ligation of imidazole to (1)$Fe^{III}(OH_2)_2$ (K_{N1}) is 10^1–10^2-fold larger than the corresponding

(16) Zhang, H.-Y.; Blasko, A.; Yu, J.-Q.; Bruice, T. C. *J. Am. Chem. Soc.* **1992**, *114*, 6621.

K_{N1} value for the ligation of ammonia, and the equilibrium constant ($K_{N1}K_{N2}$) for bis ligation of imidazole to (1)$Fe^{III}(OH_2)_2$ is 10^4-fold greater. Thus a significant fraction of the total molarity of iron(III) porphyrin is sequestered as the unreactive bis-ligated (1)Fe^{III}(imidazole)$_2$ complex before kinetically significant concentrations of mono imidazole ligated porphyrin can accumulate. This is manifested in the difference in the kinetics of reaction when employing ammonia and imidazole (compare Figures 9B and 10). Even at the very lowest concentrations of imidazole, no net rate acceleration is observed because the attenuation of rate caused by sequestering the iron(III) porphyrin as the unreactive (1)-Fe^{III}(imidazole)$_2$ overpowers any possible rate increase due to the formation of the mono nitrogen base ligated (1)$Fe^{III}(OH_2)$(imidazole). On further addition of imidazole, the rate of reaction continues to decrease until there is no reaction because all of the iron(III) porphyrin is present as (1)Fe^{III}(imidazole)$_2$. Since nitrogen base ligated porphyrin *does* represent a significant fraction of the total porphyrin, at even the lowest concentrations of imidazole added the dependence of the first-order rate constants on $[Im]_T$ is given by eq 8. The constants used for the fitting of eq 8 to the points of Figure 10 are in the Results section. It is seen that the pH-dependent binding constants obtained from the kinetic experiments ($K_1 = 2 \times 10^3$ M^{-1}, $K_2 = 6 \times 10^7$ M^{-2}) compare favorably with those obtained from the binding studies [$K_1 = (0.4–3) \times 10^3$ M^{-1}, $K_2 = (2–3) \times 10^7$ M^{-2}].

The Question of General-Acid or General-Base Catalysis by Ammonia and Amines. Scheme II only takes into account catalysis due to nitrogen base ligation to iron(III) porphyrin. The additional or alternative roles of general-acid or general-base catalysts are now considered. General-acid (by Am·H^+) or general-base (by Am) catalysis of the breakdown of the nitrogen base ligated intermediates III and $IIIH^+$ (Scheme II) requires second-order dependence of k_p on [Am]. The dependence of k_p on $[Am]_T$ = [Am·H^+] + [Am] never exceeds first order. Thus, plots of k_p vs $[Am]_T$ are linear and follow eq 7 over a 10-fold range of $[Am]_T$, and the intercepts (k_{ly}) obtained from these plots are the same as k_{ly} values obtained for the reaction of (1)$Fe^{III}(X)_2$ with *t*-BuOOH in the absence of nitrogen base.

Since general-acid or general-base catalysis by Am·H^+ or Am of the breakdown of IIH_2^+ or IIH (Scheme II), respectively, would be first order in $[Am]_T$, this possibility must be considered. However, such catalysis would be unprecedented for this system. Prior investigations of the effect of several oxygen bases and nonligating nitrogen bases upon the reactions of (1)$Fe^{III}(X)_2$ with *t*-BuOOH, (Ph)$(CH_3)_2$COOH, and (Ph)$_2$$(CH_3OCO)$COOH[14,17] have failed to reveal any catalysis by either oxygen bases or nonligating nitrogen bases. Similar results were obtained from investigations of the reactions of (2)$Fe^{III}(X)_2$,[18] (1)$Mn^{III}(X)_2$,[10,19] or (2)$Mn^{III}(X)_2$[10] with the hydroperoxides *t*-BuOOH, (Ph)-$(CH_3)_2$COOH, and (Ph)$_2$$(CH_3OCO)$COOH. Plausible general catalysis has only been observed by nonligating neutral nitrogen bases in the reactions of HOOH with (1)$Fe^{III}(OH_2)_2$[20] and (2)-$Fe^{III}(OH_2)_2$.[21] However, the hydrogen peroxide reactions differ mechanistically from the reactions with alkyl hydroperoxides in that formation of (Porph)$Fe^{III}(H_2O_2)(H_2O)$ is preequilibrium while formation of (Porph)$Fe^{III}(RO_2H)(H_2O)$ is steady state. Therefore, this reaction is much more likely to benefit from general-acid or general-base catalysis. Hydrogen peroxide is also different from alkyl hydroperoxides in that it has two dissociable protons. Thus an alternative mechanism for base catalysis involving preassociation of base to the second proton is also possible.

The following considerations show that the interpretation of the results of this study in terms of general-base catalysis by NH_3 of the breakdown of IIH_2^+ is impossible. The reactions where NH_3 acts to promote the reaction of iron(III) porphyrin with *t*-BuOOH by ligation (eq 11) or by acting as a general-base catalyst (eq 12) are kinetically equivalent. Since [(1)Fe^{III}(O-

$$v = k_{Lig}[(1)Fe^{III}(OH_2)(Am)][t\text{-BuOOH}] \quad (11)$$

$$v = k_{gb}[(1)Fe^{III}(OH_2)_2][Am][t\text{-BuOOH}] \quad (12)$$

H_2)(Am)] = K_{N1}[(1)$Fe^{III}(OH_2)_2$][Am], it follows that $k_{gb} = k_{Lig}K_{N1} = 1.1 \times 10^6$ M^{-2} s^{-1}. The rate constant k_{Lig} pertains to the reaction of eq 11, and the rate constant k_{gb} pertains to the reaction of eq 13. At 1 M NH_3, the calculated rate constant for general-base catalysis of the breakdown of IIH_2^+ (eq 13) is 1.1×10^6 M^{-1} s^{-1}, which is 10^3 greater than the rate constant realized upon full ionization of $IIH_2^+ \rightarrow$ IIH (see ref 22a). Thus, full dissociation of the H^+ would provide a smaller rate enhancement than would partial proton transfer via a general-base-catalyzed reaction. The general-base mechanism is, therefore, incompetent.

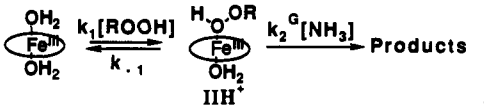

(13)

Oxyanion bases do not serve as catalysts in the reactions of (1)$M^{III}(X)_2$ [where M = Fe or Mn, and X = OH^- or H_2O] with HOOH, alkyl hydroperoxides, or acyl hydroperoxides. This may be due to an electrostatic shielding of the metal center by the negatively charged sulfonato groups on the tetraphenylporphyrin periphery. The net charge at the Fe^{III} center of (1)$Fe^{III}(X)_2$ was determined to be −1 at low pH and −2 at high pH.[14] Thus, the approach of anionic bases would be hindered by electrostatic repulsion and cause the association constants for these bases to be lowered. This interpretation is supported by the studies of Lindsay Smith and Lower[23] on the reactions of a positively charged [[5,10,15,20-tetrakis(*N*-methyl-4-pyridyl)porphyrinato]iron(III) pentachloride] with *t*-BuOOH in aqueous solution, where the rates of the reaction depend on the nature of the anionic buffer used. This would explain our observations that, while rate enhancements are observed on substituting one H_2O ligand on the Fe^{III} porphyrin by OH^- or by NH_3, no catalysis by ligation of the buffer bases $ClCH_2COO^-$, CH_3COO^-, $H_2PO_4^-$, HPO_4^{2-}, HCO_3^-, and CO_3^{2-} was observed.

Acknowledgment. This work was supported by a grant from the National Institutes of Health.

Appendix

Derivation of the Expression for Mono and Bis Ligation of Nitrogen Bases to (1)$Fe^{III}(X)_2$ (See Scheme I). In all experiments, $[Am]_T \gg [(1)Fe^{III}(X)(Y)]$ so that the mass balance for the nitrogen base is represented by eq 14, where $[Am]_T$ is the total concentration of nitrogen base and its conjugate acid.

$$[Am]_T = [AmH^+] + [Am] \quad (14)$$

$[Fe]_f$ represents the concentration of iron(III) porphyrin bearing H_2O or OH^- as axial ligands:

$$[Fe]_f = [(1)Fe^{III}(OH_2)_2] + [(1)Fe^{III}(OH_2)(OH)] \quad (15)$$

From Scheme I:

$$K_{N1} = [(1)Fe^{III}(OH_2)(Am)]/[(1)Fe^{III}(OH_2)_2][Am] \quad (16)$$

$$K_{N3} = [(1)Fe^{III}(OH)(Am)]/[(1)Fe^{III}(OH)(OH_2)][Am] \quad (17)$$

From eqs 14–17, it follows that

(17) Gopinath, E.; Bruice, T. C. *J. Am. Chem. Soc.* **1991**, *113*, 6090.
(18) Murata, K.; Panicucci, R.; Gopinath, E.; Bruice, T. C. *J. Am. Chem. Soc.* **1990**, *112*, 6072.
(19) Arasasingham, R. D.; Jeon, S.; Bruice, T. C. *J. Am. Chem. Soc.* **1992**, *114*, 2536.
(20) Lindsay Smith, J. R.; Balasubramanian, P. N.; Bruice, T. C. *J. Am. Chem. Soc.* **1988**, *110*, 7411.
(21) Panicucci, R.; Bruice, T. C. *J. Am. Chem. Soc.* **1990**, *112*, 6063.

(22) (a) The rate constant obtained upon full ionization of IIH_2^+ to IIH (Scheme II) is equal to $k_1k_4/(k_4 + k_{-3})$. A value of 1.3×10^3 M^{-1} s^{-1} is calculated for this term, from Table I of ref 13 (p 4661), since it is equal to the product of the kinetic terms $k_1k_2/(k_2 + k_{-1})$ and $(k_4/k_2)K_{a3}$ divided by the term $(k_4 + k_{-3})K_{a3}/(k_2 + k_{-1})$. (b) The rate constant obtained upon full ionization of (1)$Fe^{III}(OH_2)_2$ to (1)$Fe^{III}(OH_2)(OH)$ (Scheme II) is equal to $k_3k_4/(k_4 + k_{-3})$. A value of 0.57×10^3 M^{-1} s^{-1} is calculated for this term, from Table I of ref 13 (p 4661), since it equals the product of the kinetic terms $k_1k_2/(k_2 + k_{-1})$, $(k_4/k_2)K_{a3}$, and k_3/k_1 divided by $(k_4 + k_{-3})K_{a3}/(k_2 + k_{-1})$.
(23) Lindsay Smith, J. R.; Lower, R. J. *J. Chem. Soc., Perkin Trans. 2* **1991**, 32.

$$[(1)Fe^{III}(OH_2)(Am)] = \frac{K_{N1}K_B a_H [Fe]_f [Am]_T}{(K_{a1} + a_H)(K_B + a_H)} \quad (18)$$

$$[(1)Fe^{III}(OH)(Am)] = \frac{K_{N3}K_B K_{a1} [Fe]_f [Am]_T}{(K_{a1} + a_H)(K_B + a_H)} \quad (19)$$

The equilibrium concentration of mono nitrogen base ligated porphyrin $[Fe_N]$ then is given by

$$[Fe_N] = [(1)Fe^{III}(OH_2)(Am)] + [(1)Fe^{III}(OH)(Am)] = K_1[Fe]_f[Am]_T \quad (20a)$$

where

$$K_1 = \frac{K_B(K_{N1}a_H + K_{N3}K_{a1})}{(K_{a1} + a_H)(K_B + a_H)} \quad (20b)$$

Also from Scheme I:

$$K_{N1}K_{N2} = [(1)Fe^{III}(Am)_2]/[(1)Fe^{III}(OH_2)_2][Am]^2 \quad (21)$$

From eqs 14, 15, and 21, it follows that

$$[(1)Fe^{III}(Am)_2] = K_2[Fe]_f[Am]_T^2 \quad (22a)$$

where

$$K_2 = \frac{K_{N1}K_{N2}K_B^2 a_H}{(K_{a1} + a_H)(K_B + a_H)^2} \quad (22b)$$

Mass balance for $[(1)Fe(X)(Y)]$ is then given by

$$[Fe]_T = [Fe]_f + [Fe_N] + [(1)Fe^{III}(Am)_2] = (1 + K_1[Am]_T + K_2[Am]_T^2)[Fe]_f \quad (23)$$

The total absorbance of the solution (A_t) is a sum of the products of the extinction coefficients with the respective concentrations of each component of the solution:

$$A_t = \epsilon_1[(1)Fe^{III}(OH_2)_2] + \epsilon_2[(1)Fe^{III}(OH_2)(OH)] + \epsilon_{1N}[(1)Fe^{III}(OH_2)(Am)] + \epsilon_{2N}[(1)Fe^{III}(OH)(Am)] + \epsilon_{NN}[(1)Fe^{III}(Am)_2] \quad (24)$$

From eqs 15, 20, 21, 23, and 24, it follows that

$$A_t = \frac{(C_1 + C_2K_1[Am]_T + C_3K_2[Am]_T^2)[Fe]_T}{1 + K_1[Am]_T + K_2[Am]_T^2} \quad (25a)$$

where

$$C_1 = \frac{(\epsilon_1 a_H + \epsilon_2 K_{a1})}{(K_{a1} + a_H)} \qquad C_2 = \frac{(\epsilon_{1N}a_H + \epsilon_{2N}K'_{a1})}{(K_{a1} + a_H)} \qquad C_3 = \epsilon_{NN} \quad (25b)$$

Derivation of Kinetic Expressions for Oxidation of $(1)Fe^{III}(X)_2$ by *t*-BuOOH Catalyzed by Ammonia, TFEA, and Imidazole. Scheme II shows the proposed series of reactions where products arise from the decomposition of the intermediates IIH_2^+, IIH, $IIIH^+$, and III:

$$v = \frac{-d[t\text{-BuOOH}]}{dt} = k_2[IIH_2^+] + k_4[IIH] + k'_2[IIIH^+] + k'_4[III] \quad (26)$$

The sum of the concentrations of intermediates is given by $[II]_t = [IIH_2^+] + [IIH]$ and $[III]_t = [IIIH^+] + [III]$. The concentration of each is expressed as a mole fraction of either $[II]_t$ or $[III]_t$ and substituted into eq 26 to yield

$$v = \frac{(k_2a_H + k_4K_{a3})[II]_t}{(K_{a3} + a_H)} + \frac{(k'_2a_H + k'_4K'_{a3})[III]_t}{(K'_{a3} + a_H)} \quad (27)$$

If $[II]_t$ and $[III]_t$ are at a steady state over most of the reaction, then $[II]_t$ and $[III]_t$, respectively, are given by

$$[II]_t = \frac{(k_1a_H + k_3K_{a1})(K_{a3} + a_H)[ROOH][Fe]_f}{(K_{a1} + a_H)[(k_2 + k_{-1})a_H + (k_4 + k_{-3})K_{a3}]} \quad (28)$$

$$[III]_t = \frac{k'_1a_H(K'_{a3} + a_H)K_{N1}K_B[Am]_f[ROOH][Fe]_f}{(K_{a1} + a_H)[(k'_2 + k'_{-1})a_H + k'_4K'_{a3}](K_B + a_H)} \quad (29)$$

where $[Am]_f$ and $[Fe]_f$ are the concentrations of uncomplexed nitrogen base and $(1)Fe^{III}(X)(Y)$, respectively. However, at the concentrations of NH_3 and TFEA used in the bulk of the kinetic studies, only a very small fraction of the total $[(1)Fe^{III}(X)(Y)]$ and an even smaller fraction of total nitrogen base are present as the nitrogen base ligated species, such that $[Am]_f = [Am]_T$ and $[Fe]_f = [Fe]_T$. Equation 30 then follows from eqs 27–29:

$$\frac{v}{[ROOH][Fe]_T} = k_p = k_{ly} + k_{BT}[Am]_T \quad (30a)$$

where

$$k_{ly} = \frac{\frac{k_1k_2}{(k_2 + k_{-1})}\left\{a_H + \frac{k_4}{k_2}K_{a3}\right\}\left\{a_H + \frac{k_3}{k_1}K_{a1}\right\}}{(K_{a1} + a_H)\left\{a_H + \frac{(k_4 + k_{-3})}{(k_2 + k_{-1})}K_{a3}\right\}} \quad (30b)$$

$$k_{BT} = \frac{\frac{k'_1k'_2}{(k'_2 + k'_{-1})}K_{N1}K_B a_H\left\{a_H + \frac{k'_4}{k'_2}K'_{a3}\right\}}{(K_{a1} + a_H)(K_B + a_H)\left\{a_H + \frac{k'_4}{(k'_2 + k'_{-1})}K'_{a3}\right\}} \quad (30c)$$

However, at the concentrations of imidazole used in the kinetic experiments, or at high concentrations of ammonia, $[Am]_f = [Am]_T$, but $[Fe]_f$ is given by eq 23. Therefore, the kinetic expression for imidazole-catalyzed reaction is given by

$$k_p = \frac{k_{ly} + k_{BT}[Am]_T}{1 + K_1[Am]_T + K_2[Am]_T^2} \quad (31)$$